PHYSICAL REVIEW C **85**, 064329 (2012)

Neutron shell structure and deformation in neutron-drip-line nuclei

Ikuko Hamamoto[1,2,*]
[1]*Riken Nishina Center, Wako, Saitama 351-0198, Japan*
[2]*Division of Mathematical Physics, Lund Institute of Technology at the University of Lund, Lund, Sweden*
(Received 17 May 2012; published 27 June 2012)

Neutron shell structure and the resulting possible deformation in the neighborhood of neutron-drip-line nuclei are systematically discussed, based on both bound and resonant neutron one-particle energies obtained from spherical and deformed Woods-Saxon potentials. Owing to the unique behavior of weakly bound and resonant neutron one-particle levels with smaller orbital angular momenta ℓ, a systematic change in the shell structure and thereby a change in the neutron magic numbers are pointed out, compared with those of stable nuclei expected from the conventional *j-j* shell model. For a spherical shape with the operator of the spin-orbit potential conventionally used, the ℓ_j levels belonging to a given oscillator major shell with parallel spin and orbital angular momenta tend to gather together in the energetically lower half of the major shell, while the levels with antiparallel spin and orbital angular momenta gather in the upper half. This tendency leads to a unique shell structure and possible deformation when neutrons start to occupy the orbits in the lower half of the major shell. Among others, the neutron magic number $N = 28$ disappears and $N = 50$ may disappear, while the magic number $N = 82$ may presumably survive owing to the large $\ell = 5$ spin-orbit splitting for the $1h_{11/2}$ orbit. On the other hand, an appreciable amount of energy gap may appear at $N = 16$ and 40 for spherical shape, while neutron-drip-line nuclei in the region of neutron numbers above $N = 20$, 40, and 82, namely, $N \approx 21$–28, $N \approx 41$–54, and $N \approx 83$–90, may be quadrupole deformed, although the possible deformation also depends on the proton number of the respective nuclei.

DOI: 10.1103/PhysRevC.85.064329 PACS number(s): 21.60.Ev, 21.10.Pc, 21.90.+f

I. INTRODUCTION

Thanks to the development of various facilities of radioactive nuclear ion beams, the knowledge of nuclei far away from the stability line has recently been much increased. Though the neutron drip line has so far been experimentally pinned down up to the oxygen isotope (proton number $Z = 8$), at the moment the experimental knowledge of nuclei with $Z > 8$ close to the neutron drip line is quickly increasing.

The study of unstable nuclei, especially neutron-drip-line nuclei which contain very weakly bound neutrons, has opened a new field in the study of the structure of finite quantum-mechanical systems. The study is important not only because of the interests in nuclear astrophysics, namely, understanding the production of energy and the synthesis of elements in stars and during stellar events, but also because it provides the opportunity to learn the properties of a fermion system with very loosely bound particles, some density of which can extend to the region far outside the region of the main density of the system. Various exciting studies of manmade finite quantum-mechanical systems, such as clusters of atoms and quantum dots, have recently been made possible, however, these systems have so far been limited to be well bound so that the related potentials are in a good approximation simulated by a harmonic oscillator. Because the nucleon separation energy in stable nuclei is 7–10 MeV, the spectroscopic analysis around the ground state of stable nuclei has been successfully carried out also in terms of harmonic-oscillator wave functions. Correspondingly, most systematic nuclear shell-model calculations have so far been carried out using harmonic-oscillator wave functions.

The study of one-particle motion in deformed potentials is the basis for understanding the structure of deformed nuclei. Because the Fermi level of drip-line nuclei lies close to the continuum, both weakly bound and positive-energy one-particle levels play a crucial role in the many-body correlations of those nuclei. Among an infinite number of one-particle levels at a given positive energy, only some selected levels related to one-particle resonant levels will be important for the understanding of the properties of bound states of drip-line nuclei.

The behavior of *s* neutrons is an extreme example because the barrier coming from either centrifugal or Coulomb potentials is absent. Therefore, for example, as the separation energy approaches 0, the probability of *s* neutrons staying inside the nuclei approaches 0. When a larger part of a bound one-particle wave function lies outside the nuclear potential, the one-particle eigenenergy becomes less sensitive to the potential provided by the well-bound nucleons in the system. In contrast, the wave functions of weakly bound but large-ℓ neutrons stay mostly inside the nuclear potential, owing to the high barrier coming from the centrifugal potential, of which the height is proportional to $\ell(\ell + 1)$. Consequently, when the potential changes (or the neutron number for a given proton number approaches the neutron drip line) so that the one-particle energies of the last bound neutrons approach 0, the binding energy of larger-ℓ neutrons, which is more sensitive to the strength of the potential, decreases much more rapidly than that of smaller-ℓ neutrons. The height of the centrifugal potential also greatly affects the properties of one-particle resonant levels. Thus, the same behavior of ℓ dependence as

*ikuko@matfys.lth.se

that of weakly bound neutron energies is also obtained for lower-lying neutron one-particle resonant energies, as shown in Refs. [1–3]. This ℓ-dependent behavior of one-particle energies on the potential strength leads to a systematic change in the shell structure in both weakly bound and resonant neutron one-particle energies compared with the shell structure of strongly bound neutrons [4].

Using the numerical result of self-consistent mean-field calculations with effective interactions used in stable nuclei while limiting the spherical system to a large box, one-particle spectra of bound nucleons in spherical drip-line nuclei were studied in Ref. [5]. And some systematic change in shell structure in bound neutron energies of spherical neutron drip-line nuclei was obtained, which is similar to that in the present work found at $\beta = 0$ except for the conclusion in Ref. [5] that the presence of magic gaps at neutron numbers $N = 28$, 50, and 82 does not appreciably change as one approaches the neutron drip line.

Taking the $(N = 2)$ sd shells and $(N = 3)$ pf shells, where N expresses the harmonic-oscillator principle quantum number, the systematic change in shell structure owing to the unique behavior of one-particle energies of weakly bound or resonant levels with small ℓ is briefly explained in the following. In stable sd-shell nuclei, it is well known that the relation of one-particle energies is such that $\epsilon(1d_{5/2}) < \epsilon(2s_{1/2}) < \epsilon(1d_{3/2})$, which agrees with experimental information. However, in lighter neutron-rich nuclei, in which the $2s_{1/2}$ level becomes very weakly bound, the relation $\epsilon(2s_{1/2}) \approx \epsilon(1d_{5/2}) < \epsilon(1d_{3/2})$ is expected, which leads to the new magic number $N = 16$ [6]. In fact, the appearance of the $N = 16$ neutron magic number for unstable nuclei together with the weakening of the shell closure at $N = 20$ and 28 was mentioned in 1975 [7] based on the self-consistent calculations using the energy density formalism with pairing interaction. On the other hand, in heavier nuclei where neutrons in the sd-shell are strongly bound, the relation $\epsilon(1d_{5/2}) < \epsilon(1d_{3/2}) < \epsilon(2s_{1/2})$ is obtained from both Hartree-Fock (HF) calculations and eigenvalues of Woods-Saxon potentials with a practical strength of spin-orbit potential. Similarly, if we take an example of the pf shell, the relation $\epsilon(1f_{7/2}) < \epsilon(1f_{5/2}) < \epsilon(2p_{3/2}) < \epsilon(2p_{1/2})$ is obtained in the case of strongly bound pf neutrons. For stable pf-shell nuclei, the relation $\epsilon(1f_{7/2}) < \epsilon(2p_{3/2}) < \epsilon(1f_{5/2}) \approx \epsilon(2p_{1/2})$ is known. However, when one-particle levels of $1f_{7/2}$ and $2p_{3/2}$ become very weakly bound or resonant, the relation $\epsilon(1f_{7/2}) \approx \epsilon(2p_{3/2})$ appears. The relation leads to the disappearance of the magic number $N = 28$ [4], and moreover, nuclei with some neutrons in the almost-degenerate $f_{7/2}$ and $p_{3/2}$ shells, which couple strongly to each other by quadrupole-quadrupole interaction, may be easily quadrupole deformed. The degeneracy can well be responsible for the presence of the island of inversion. It is known that the presence of only like nucleons in a large single j shell can hardly lead to quadrupole deformation. On the other hand, the presence of like nucleons in several nearly degenerate j shells, which couple strongly to each other by quadrupole-quadrupole interaction, may lead to quadrupole deformation.

In axially symmetric quadrupole-deformed nuclei the role of smaller-ℓ neutrons in a spherical shape is replaced by neutrons with smaller Ω values, where Ω denotes the angular momentum component of neutrons along the axially symmetry axis. For example, the smallest possible angular momentum component of $\Omega^\pi = 1/2^+$ orbits is $s_{1/2}$, which always becomes the overwhelming component of angular momentum in neutron one-particle wave functions with $\Omega^\pi = 1/2^+$ as the binding energy of the neutron approaches 0 [1,8]. In the case where the smallest orbital angular momentum is not equal to 0, it depends on the properties of the respective orbits how the component of the smallest orbital angular momentum becomes dominant in one-particle wave functions when the binding energy approaches 0 [1]. Because all spherical one-particle orbits with positive parity ($s_{1/2}, d_{3/2}, d_{5/2}, \ldots$) have an $\Omega^\pi = 1/2^+$ component, the shell structure change for a deformed shape close to the continuum owing to the unique property of an $s_{1/2}$ orbit is expected to occur more often compared with the case of a spherical shape. The most convenient way to see the shell structure of deformed nuclei is to plot one-particle energies as a function of quadrupole deformation (Nilsson diagram) [9]. Therefore, in this article Nilsson diagrams that are relevant to some possible neutron-drip-line nuclei related to neutron magic numbers in stable nuclei are presented. The change in nuclear shell structure for neutrons is seen in both bound and resonant one-particle energies in Nilsson diagrams.

In Sec. II the main points of our model are briefly summarized, while numerical results are presented in Sec. III. Conclusions and discussions are given in Sec. IV.

II. MODEL

In order to solve the eigenvalue [1] and eigenphase [2,3] problems for neutron one-particle bound and resonant levels, respectively, as a function of axially symmetric quadrupole deformation, the coupled differential equations obtained from the Schrödinger equation are integrated in coordinate space with correct asymptotic behavior at $r = R_{\max}$, where $R_{\max}$ is so large that both the nuclear potential and the coupling term are negligible. In this way one-particle resonant energy in deformed nuclei can also be estimated without any ambiguity. For $\beta \neq 0$ the resonant energy is defined as the energy at which one of the eigenphases increases through $\pi/2$ as the energy increases [2,3,10]. One-particle resonance is absent if none of the eigenphases increases through $\pi/2$ as the energy increases. For example, a neutron one-particle resonant state with $\Omega^\pi = 1/2^+$ is not obtained as long as the major component of the one-particle wave function comes from $\ell = 0$, because an $\Omega^\pi = 1/2^+$ level with an appreciable amount of the $\ell = 0$ component can very quickly decay via the $\ell = 0$ channel. Because the height of the centrifugal barrier decreases for a larger nuclear radius, the unique behavior of $\ell = 1$ components contained in the $\Omega^\pi = 1/2^-$ and $3/2^-$ orbits will be more easily seen in heavier nuclei.

On the other hand, because the height of the centrifugal barrier is proportional to $\ell(\ell + 1)$, at a given positive energy for a given potential the width of a one-particle resonant level is larger for a level with a smaller orbital angular momentum. As the energy increases, the width of a given resonant level becomes larger, and finally, at a certain energy the one-particle level with a given ℓ is no longer obtained as a resonant level.

For simplicity, the calculated widths of one-particle resonant levels are not given in the present article, as the widths are not of major interest in this work.

Though weakly bound neutrons in nuclei close to the neutron drip line make a contribution especially to the tail of the self-consistent nuclear potentials, the major part of the nuclear potential is provided by well-bound nucleons, especially by strongly bound protons in the case of neutron-rich nuclei. Therefore, for simplicity, in this article the parameters of Woods-Saxon potentials are taken from the standard ones (see p. 239 of Ref. [11]). Namely, the diffuseness $a = 0.67$ fm, the radius $r_0 A^{1/3}$ where $r_0 = 1.27$ fm, the depth of the Woods-Saxon potential for neutrons is

$$V = -51 + 33\frac{N-Z}{A} \quad \text{(MeV)}, \tag{1}$$

and the spin-orbit potential is expressed by

$$V_{\ell s} = -0.44V(\vec{\ell}\cdot\vec{s})r_0^2\frac{1}{r}\frac{d}{dr}f(r) \quad \text{(MeV)}, \tag{2}$$

where

$$f(r) = \frac{1}{1+\exp(\frac{r-R}{a})}. \tag{3}$$

It is noted that the neutron potential for nuclei with a neutron excess is shallower than that for $N = Z$ nuclei. In fact, the nuclear potential with the above set of parameters is found to approximately reproduce the position of the neutron drip line, which is expected from presently available experimental data.

In the discussion of the possible deformation of given nuclei examining the Nilsson diagram, we use the following empirical facts: (a) if pair correlation plays a minor role, the presence of neutrons in almost-degenerate ℓ_j shells around the Fermi level may make the system deformed, as those neutrons have the possibility of gaining energy by breaking spherical symmetry (Jahn-Teller effect); (b) in order to obtain a deviation from a spherical shape, the energies of one-particle levels just below and on the Fermi level in the Nilsson diagram need to be mostly decreasing (downward-going) for $\beta = 0 \to \beta \neq 0$ so that the system gains the energy by deformation [9]; (c) the presence of only like nucleons in a large single j shell may not be sufficient to deform the system, although the presence of both neutrons and protons in a given single j shell may induce some quadrupole deformation (examples are the absence of observed deformed nuclei in both the $_{38}$Sr and the $_{40}$Zr isotopes, owing to the occupation of the $1g_{9/2}$ shell by neutrons [12], and in the $_{18}Ar$ and $_{20}$Ca isotopes, owing to the occupation of the $1f_{7/2}$ shell by neutrons); and (d) only prolate deformation is discussed, as it is empirically known that prolate deformation is overwhelmingly dominant among deformed nuclei, although the absolute dominance is not yet fully understood [13].

III. NUMERICAL RESULTS

Though the near-degeneracy of both the $1d_{5/2} - 2s_{1/2}$ levels in the $N = 2$ oscillator shell and that of the $1f_{7/2} - 2p_{3/2}$ levels in the $N = 3$ shell of the spherical potential in neutron-drip-line nuclei as well as the resulting possible deformation are partially discussed in Ref. [4], in the following we include a brief description of these cases for completeness. The two remaining $n\ell_j$ levels, $1f_{5/2}$ and $2p_{1/2}$, in the $N = 3$ oscillator major shell other than the $1f_{7/2}$ and $2p_{3/2}$ levels, in which spin and orbital angular momenta are antiparallel, may also become almost degenerate around the Fermi level of certain nuclei. Nevertheless, the degeneracy may not lead to a deformation, because these levels lie in the second half of the $N = 3$ major shell, and thus, the general behavior of the deformed one-particle energies originating from these levels in the spherical limit is energetically upward-going for $\beta = 0 \to \beta \neq 0$. The relation between deformation of the system and upward-going (or downward-going) energy levels in the Nilsson diagram is known already from the study of stable rare-earth nuclei [9]. Namely, energetically downward-going one-particle levels for $\beta = 0 \to \beta > 0$ (prolate shape) around $N \gtrsim 88$–90, which lead to stable deformed rare-earth nuclei, end at $N \approx 110$, around which the observed deformation of stable rare-earth nuclei also ends. (See, e.g., Fig. 5-3 in Ref. [9].) As shown in the following, the shell structure unique in neutron weakly bound and resonant levels leads to the bunching of one-particle levels in a given N major shell for a spherical shape: levels with parallel spin and orbital angular momenta gather together in the lower half of the major shell, while levels with antiparallel spin and orbital angular momenta gather in the upper half-shell. Levels within the respective groups couple with each other strongly by spin-independent quadrupole-quadrupole interaction. However, we note that there is a difference between the two groups concerning the possible deformation. Namely, having neutrons in the nearly degenerate levels with parallel spin and orbital angular momenta may make the system deformed, because one-particle energies in the lower half of a given N major shell are, in general, decreasing for $\beta = 0 \to \beta \neq 0$, as can be seen from the Nilsson diagram. Because the levels belonging to each group have different orbital angular momenta, the occurrence of near-degeneracy depends on the actual strength of spin-orbit splitting and the values of relevant orbital angular momenta. As shown in the $1h_{11/2}$ orbit in Fig. 4, the highest j level with parallel spin and orbital angular momenta tends to go out of the group of degenerate levels in heavier nuclei.

A. Near-degeneracy of $1d_{5/2}$ and $2s_{1/2}$ levels

In Fig. 1 we show the Nilsson diagram for neutrons, in which parameters of the Woods-Saxon potential are chosen for the nucleus $^{18}_{6}C_{12}$. It is noted that the observed ground-state spins of nuclei $^{15}_{6}C_9$, $^{17}_{6}C_{11}$, and $^{19}_{6}C_{13}$ are $1/2^+$, $3/2^+$, and $1/2^+$, respectively, and are most easily understood in terms of prolate deformation for $\beta > 0.1$, where the last odd neutron occupies the $\Omega^\pi = 1/2^+$, $3/2^+$, and $1/2^+$ levels, which correspond to the 9th, 11th, and 13th neutron one-particle levels, respectively, assuming that the respective even-even core nucleons occupy pairwise the lower-lying Nilsson one-particle levels and couple to $I^\pi = K^\pi = 0^+$. For some experimental evidence of the deformation of these C isotopes, see Refs. [14] and [15]. At $\beta = 0$ the calculated energy difference between the $2s_{1/2}$ and the $1d_{5/2}$ levels in Fig. 1 is only 509 keV. In contrast, a large energy gap for a spherical shape ($\beta = 0$) appears at $N = 16$, as the calculated $1d_{3/2}$ resonant energy is 4.36 MeV.

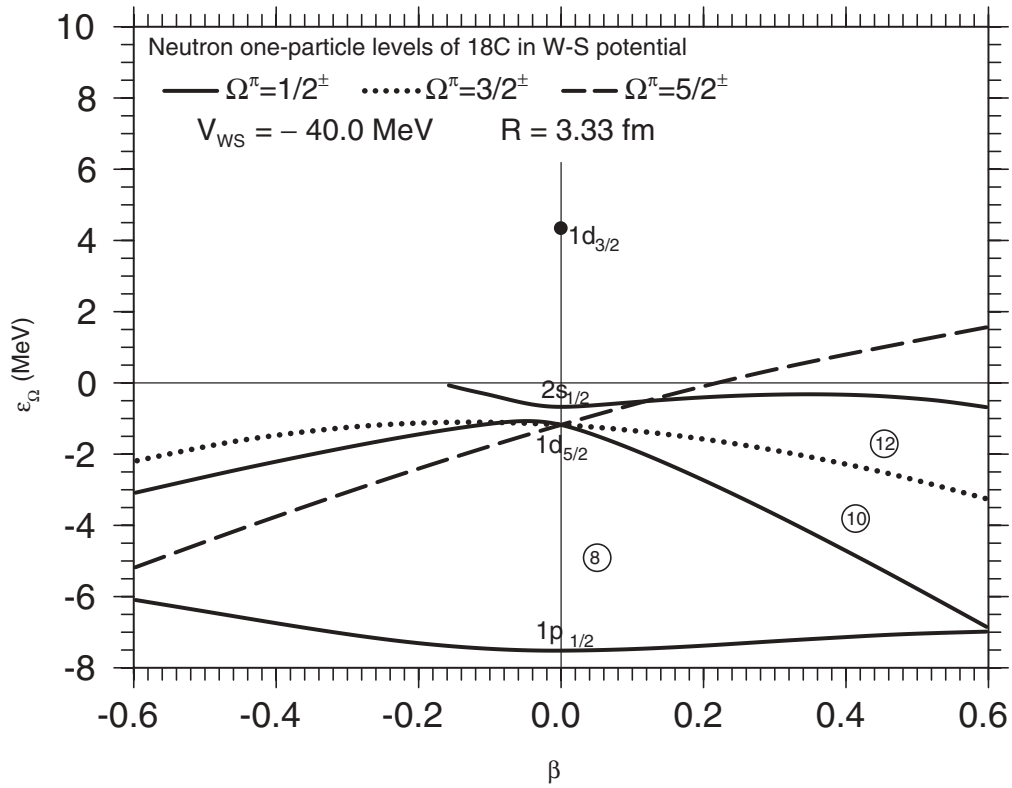

FIG. 1. Calculated neutron one-particle energies as a function of quadrupole deformation. Parameters of the Woods-Saxon potential are chosen for the nucleus $^{18}_{6}C_{12}$. Bound one-particle energies at $\beta = 0$ are -1.17 and -0.66 MeV for the $1d_{5/2}$ and $2s_{1/2}$ levels, respectively, while the one-particle resonant $1d_{3/2}$ level is obtained at $+4.36$ MeV, denoted by the filled circle. One-particle resonant levels for $\beta \neq 0$ are not plotted unless they are important in the present discussion. For simplicity, calculated widths of one-particle resonant levels are not shown. The neutron numbers, 8, 10, and 12, which are obtained by filling all lower-lying levels, are indicated by open circles. One-particle levels with $\Omega = 1/2$, $3/2$, and $5/2$ are expressed by solid, dotted, and long-dashed curves, respectively, for both positive and negative parities. The parity of levels can be seen from the ℓ values denoted at $\beta = 0$, $\pi = (-1)^{\ell}$.

B. Near-degeneracy of $1f_{7/2}$ and $2p_{3/2}$ levels

In Fig. 2 the Nilsson diagram for neutrons is shown, in which parameters of the Woods-Saxon potential are chosen for the nucleus $^{34}_{12}Mg_{22}$. At $\beta = 0$ the calculated energy difference between the very weakly bound $1f_{7/2}$ level and the very low-lying one-particle resonant $2p_{3/2}$ level is only 387 keV, which clearly indicates that the $N = 28$ energy gap at $\beta = 0$ disappears in neutron-drip-line nuclei. This near-degeneracy of the two levels, which couple strongly to each other by spin-independent quadrupole-quadrupole interaction, may lead to the deformation of a system with $N \approx 21$–28, as a result of the Jahn-Teller effect. In particular, odd-A nuclei with $N = 21$ such as $^{33}_{12}Mg_{21}$ [16,17] and $^{31}_{10}Ne_{21}$ [18] are observed to be deformed, which is consistent with the strongly down-sloping Nilsson one-particle levels with $\Omega^{\pi} = 1/2^{-}$ and $3/2^{-}$ for $\beta > 0$, which originate from the $1f_{7/2}$ shell in the spherical limit ($\beta = 0$). Neutron-drip-line nuclei with $N = 21$–28 can well be deformed, although the possible deformation also depends on the proton number of the respective nuclei. Examining the Nilsson diagram for protons, it is seen that the proton numbers $Z = 9$ (F), $Z = 10$ (Ne), $Z = 11$ (Na), and $Z = 12$ (Mg) may prefer some deformation, as the energies of the two lowest-lying Nilsson one-proton levels in the sd shell decrease sharply as $\beta = 0 \rightarrow \beta \neq 0$. The recent experimental information on the Mg isotope with $N = 21$–26 [19] seems to go well with this interpretation using the Nilsson diagram. Indeed, this near-degeneracy of the $1f_{7/2}$ and $2p_{3/2}$ levels can be an important element for creating the island of inversion. In other words, heavier nuclei in the island of inversion could survive inside the neutron drip line thanks to the deformation.

In Fig. 2 it is also shown that at $\beta = 0$ the well-bound $2s_{1/2}$ level lies approximately in the middle of the $2d_{5/2}$ and $2d_{3/2}$ levels, in contrast to the sd-shell level scheme shown in Fig. 1.

C. Near-degeneracy of $1g_{9/2}$, $3s_{1/2}$, and $2d_{5/2}$ levels

Figure 3 shows the Nilsson diagram for neutrons in which the parameters of the Woods-Saxon potential are chosen for the nucleus $^{66}_{22}Ti_{44}$. A considerable amount of energy gap appears at $N = 40$ for a spherical shape, while the possible location of the $3s_{1/2}$ level slightly above 0 (indicated by the open circle in Fig. 3) is obtained from the extrapolation of the bound one-particle energy level with $\Omega^{\pi} = 1/2^{+}$ for $\beta > 0.12$ denoted by the solid curve in Fig. 3, which reaches 0 at $\beta = 0.12$, as the continuation of the one-particle resonant level to the region of $\beta < 0.12$ cannot be obtained owing to the predominant $\ell = 0$ component of the orbit. Thus, the calculated $1g_{9/2}$, $3s_{1/2}$, and $2d_{5/2}$ levels, which are the three

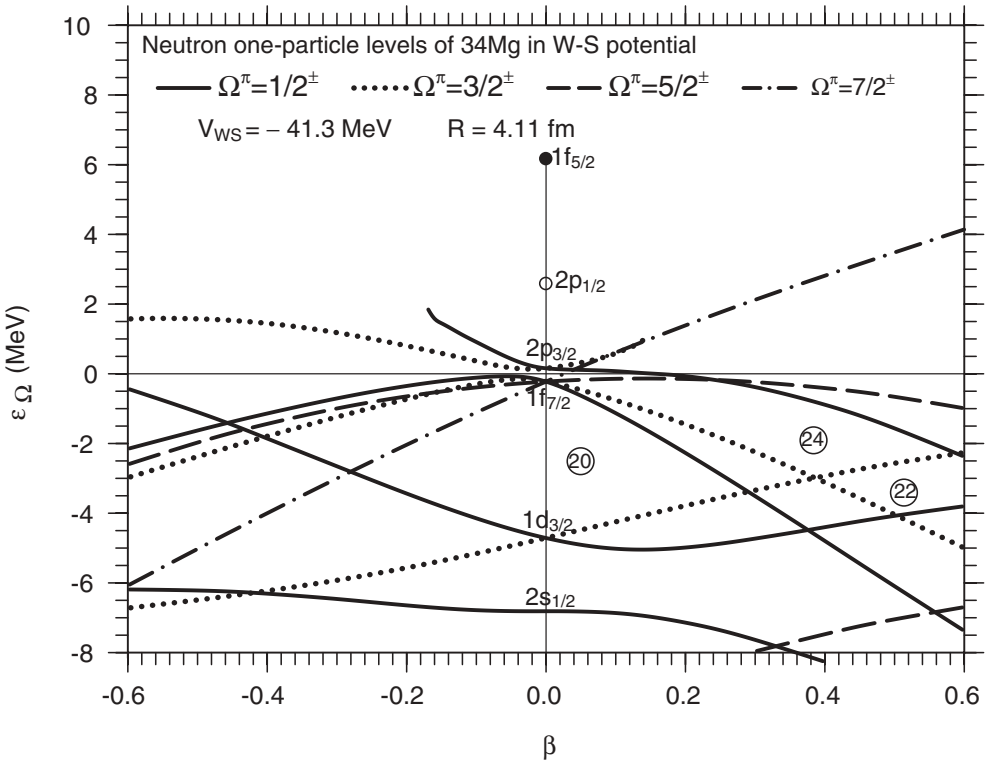

FIG. 2. Calculated neutron one-particle energies as a function of quadrupole deformation. Parameters of the Woods-Saxon potential are chosen for the nucleus $^{34}_{12}Mg_{22}$. Bound one-particle energies at $\beta = 0$ are -9.80, -6.84, -4.75, and -0.24 MeV for the $1d_{5/2}$, $2s_{1/2}$, $1d_{3/2}$, and $1f_{7/2}$ levels, respectively, while one-particle resonant $2p_{3/2}$ and $1f_{5/2}$ levels are obtained at $+0.15$ and $+6.18$ MeV, respectively. The $2p_{1/2}$ one-particle resonant level is not obtained for the present potential, however, its approximate position at $\beta = 0$ is denoted by an open circle, at which an eigenphase does not reach, but comes close to, $\pi/2$. One-particle resonant levels for $\beta \neq 0$ are not plotted unless they are important in relation to the present interests. The neutron numbers, 20, 22, and 24, which are obtained by filling all lower-lying levels, are indicated by open circles. One-particle levels with $\Omega = 1/2$, $3/2$, $5/2$, and $7/2$ are expressed by solid, dotted, long-dashed, and dot-dashed curves, respectively, for both positive and negative parities.

$n\ell_j$ levels belonging to the $N = 4$ oscillator shell with parallel spin and orbital angular momenta and couple strongly to each other by spin-independent quadrupole-quadrupole interaction, lie within 1.43 MeV. This means that the energy gap at the magic number $N = 50$ clearly disappears.

The strong quadrupole coupling of these three levels can be seen in the Nilsson diagram in Fig. 3. For example, the lowest-lying one-particle level with $\Omega^\pi = 1/2^+$ for $\beta > 0$, which is connected to the $1g_{9/2}$ shell at $\beta = 0$, contains a considerable amount of $3s_{1/2}$ and $2d_{5/2}$ components already at moderate values of β. This can be seen from the comparison of the slopes of the $\Omega^\pi = 1/2^+$ curve for $\beta > 0$ versus the $\Omega^\pi = 9/2^+$ curve for $\beta < 0$, both of which originate from the $1g_{9/2}$ level at $\beta = 0$. The wave function of the $\Omega^\pi = 9/2^+$ orbit is almost pure $1g_{9/2}$ in the present range of β values, as there is no $\Omega^\pi = 9/2^+$ one-particle orbit in the neighborhood. If both orbits, $\Omega^\pi = 1/2^+$ for $\beta > 0$ and $\Omega^\pi = 9/2^+$ for $\beta < 0$, consist only of a single j shell, namely, $g_{9/2}$, then the absolute magnitude of the slope, $|\frac{d\epsilon_\Omega}{d\beta}|$, of the $\Omega^\pi = 9/2^+$ level is a factor of 2 larger than that of the $\Omega^\pi = 1/2^+$ level. On the other hand, for a pure harmonic-oscillator potential (namely, the strong mixing limit), the former is half (=0.5) of the latter. In Fig. 3 the ratio of the former to the latter is about 2, of course, for $|\beta| \ll 1$, while the absolute magnitude of the slope of the $\Omega^\pi = 1/2^+$ energy level becomes larger than that of the $\Omega^\pi = 9/2^+$ energy level already at $|\beta| < 0.3$.

The near-degeneracy of these three levels, $1g_{9/2}$, $3s_{1/2}$, and $2d_{5/2}$, corresponds to that of the $1f_{7/2}$ and $2p_{3/2}$ levels discussed in the previous subsection, which leads to the island of inversion. First, neutron-drip-line nuclei with $N = 41$ are likely to be deformed, though the possible deformation also depends on the proton number of the respective nuclei. The ground-state spin of neutron-drip-line nuclei with $N = 41$ can be either $1/2^+$ or $5/2^+$ or $1/2^-$ or $3/2^-$, depending on the β values if they are prolately deformed, instead of the $9/2^+$ expected for a spherical shape. Second, a system having several neutrons in these ($1g_{9/2}$-$3s_{1/2}$-$2d_{5/2}$) almost-degenerate shells such as $N \approx 41$–54 is likely to be deformed in a similar way to the island of inversion when pairing interaction plays a minor role. See the fourth paragraph in Sec. IV for a discussion of the role of pairing interaction in the determination of the shape of neutron-drip-line nuclei.

Near-degeneracy of the $1g_{9/2}$ level with the other two levels has occurred for the phenomenological strength of the spin-orbit splitting, which is still not as strong for the $1g_{9/2}$ orbit. As shown in Sec. III D, in the $N = 5$ oscillator major shell the spin-orbit splitting of the $1h_{11/2}$ level is so strong that a similar degeneracy of all levels with parallel spin and orbital angular

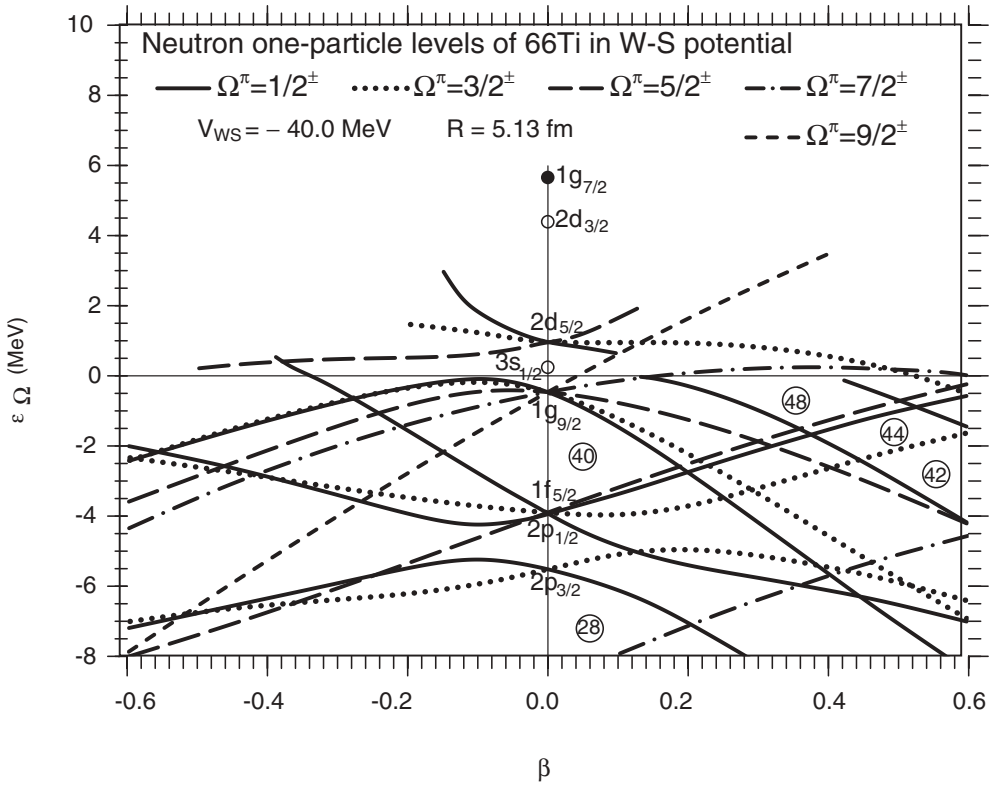

FIG. 3. Calculated neutron one-particle energies as a function of quadrupole deformation. Parameters of the Woods-Saxon potential are chosen for the nucleus $^{66}_{22}\mathrm{Ti}_{44}$. Bound one-particle energies at $\beta = 0$ are -8.82, -5.54, -3.99, -3.94, and -0.48 MeV for the $1f_{7/2}$, $2p_{3/2}$, $2p_{1/2}$, $1f_{5/2}$, and $1g_{9/2}$ levels, respectively, while one-particle resonant $2d_{5/2}$, $1g_{7/2}$, and $1h_{11/2}$ levels are obtained at $+0.96$, $+5.66$, and $+7.57$ MeV, respectively. The $2d_{3/2}$ one-particle resonant level is not obtained for the present potential, however, its approximate position at $\beta = 0$ is denoted by an open circle, at which an eigenphase does not reach, but comes close to, $\pi/2$. The $3s_{1/2}$ resonant level does not exist in any case, but the open circle at $\beta = 0$ indicates the energy obtained by extrapolating the solid curve of the bound $\Omega^\pi = 1/2^+$ orbit for $\beta > 0.12$ to $\beta = 0$, although the calculated solid curve reaches 0 at $\beta = 0.12$ and cannot continue to $\beta < 0.12$. The major component of the solid curve for $\epsilon_\Omega(<0) \to 0$ is clearly $3s_{1/2}$. One-particle resonant levels for $\beta \neq 0$ are not plotted if they are not relevant for the present discussion. The neutron numbers, 28, 40, 42, 44, and 48, which are obtained by filling all lower-lying levels, are indicated by open circles. One-particle levels with $\Omega = 1/2$, $3/2$, $5/2$, $7/2$, and $9/2$ are expressed by solid, dotted, long-dashed, dot-dashed, and short-dashed curves, respectively, for both positive and negative parities.

momenta belonging to the $N = 5$ major shell can hardly occur.

The remaining two levels in the $N = 4$ oscillator major shell, $1g_{7/2}$ and $2d_{3/2}$, may be almost degenerate around the Fermi level of certain neutron-drip-line nuclei. However, it may be difficult to gain energies by deforming those nuclei which have neutrons in those two levels, as one-particle energies originating from the $1g_{7/2}$ and $2d_{3/2}$ levels are located in the second half of the $N = 4$ major shell and thus the energies of the majority of one-particle levels increase for $\beta = 0 \to \beta \neq 0$.

D. Near-degeneracy of $1h_{11/2}$, $2f_{7/2}$, and $3p_{3/2}$ levels?

In Fig. 4 the Nilsson diagram for neutrons is shown, in which parameters of the Woods-Saxon potential are chosen for the nucleus $^{126}_{44}\mathrm{Ru}_{82}$. A considerable amount of the energy gap remains at $N = 82$ for a spherical shape owing to the large spin-orbit splitting of the $\ell = 5$ level, $1h_{11/2}$, while the very weakly bound $2f_{7/2}$ and $3p_{3/2}$ levels are very close-lying. The calculated energy distance between the two levels is only 419 keV.

The set of three levels, $1h_{11/2}$, $2f_{7/2}$, and $3p_{3/2}$, which strongly couple to each other by spin-independent quadrupole-quadrupole interaction, is the set of the $N = 5$ oscillator major shell analogous to the set of three levels, $1g_{9/2}$, $2d_{5/2}$, and $3s_{1/2}$, of the $N = 4$ major shell discussed in Sec. III C. In the latter case a deformation may be energetically preferred for a system where some neutrons occupy the set of levels owing to the Jahn-Teller effect, while in the present case a deformation may not be preferred, as the one-particle levels for a moderate size of prolate shape in Fig. 4 originating from $1h_{11/2}$ seem mostly to maintain the feature of the single j shell. On the other hand, the occupation of the almost-degenerate shells, $2f_{7/2}$ and $3p_{3/2}$, by some neutrons may lead to a deformed system for $N = 83$–90 when the proton part of the respective nuclei is energetically easily deformable and the pairing interaction plays a minor role. For example, the nucleus $^{127}_{44}\mathrm{Ru}_{83}$ may be deformed in a similar way to the nucleus $^{33}_{12}\mathrm{Mg}_{21}$ in the island of inversion (see Fig. 2.). If it is deformed, the ground-state

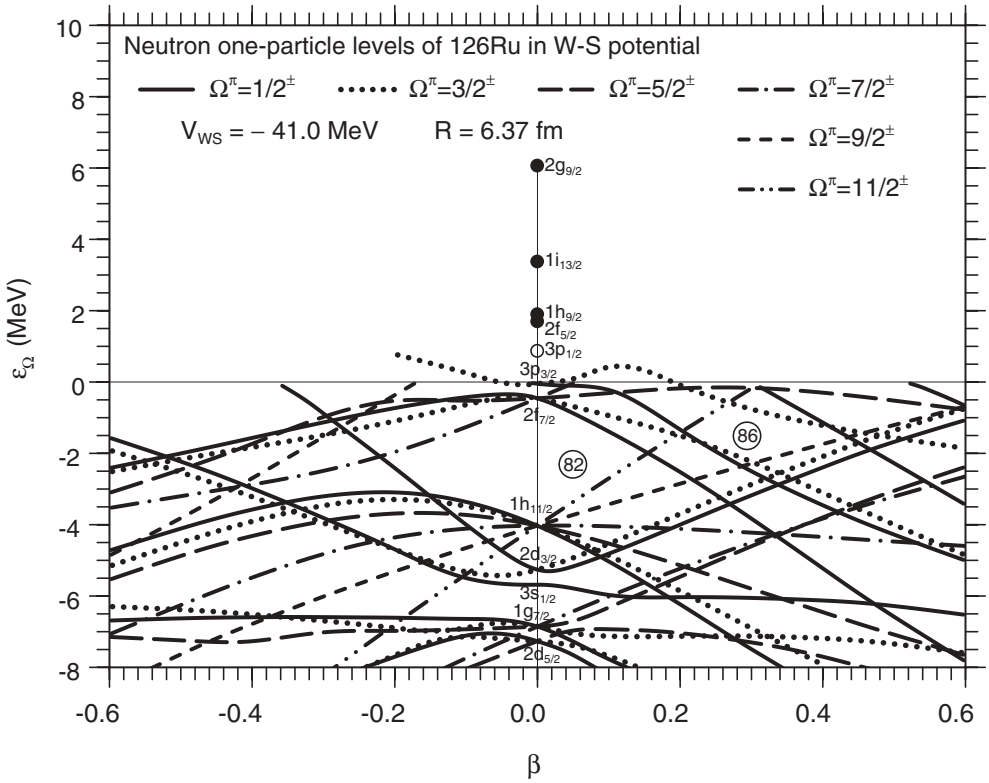

FIG. 4. Calculated neutron one-particle energies as a function of quadrupole deformation. Parameters of the Woods-Saxon potential are chosen for the nucleus $^{126}_{44}Ru_{82}$. Bound one-particle energies at $\beta = 0$ are -7.28, -6.90, -5.70, -5.29, -4.05 -0.48, and -0.06 MeV for the $2d_{5/2}$, $1g_{7/2}$, $3s_{1/2}$, $2d_{3/2}$, $1h_{11/2}$, $2f_{7/2}$, and $3p_{3/2}$ levels, respectively, while one-particle resonant $2f_{5/2}$, $1h_{9/2}$, $1i_{13/2}$, and $2g_{9/2}$ levels are obtained at $+1.71$, $+1.91$, $+3.38$, and $+6.07$ MeV, respectively. The $3p_{1/2}$ one-particle resonant level is not obtained for the present potential, but the open circle at $\beta = 0$ indicates the energy obtained by calculating the spin-orbit splitting of the $\ell = 1$ levels from that of the $\ell = 3$ ($2f_{5/2}$ and $2f_{7/2}$) levels and using the calculated energy of the $3p_{3/2}$ level. One-particle resonant levels for $\beta \neq 0$ are not plotted if they are not relevant for the present discussion. The neutron numbers 82 and 86, which are obtained by filling all lower-lying levels, are indicated by open circles. One-particle levels with $\Omega = 1/2$, $3/2$, $5/2$, $7/2$, $9/2$, and $11/2$ are expressed by solid, dotted, long-dashed, dot-dashed, short-dashed, and dot-dot-dashed curves, respectively, for both positive and negative parities.

spin of the $N = 83$ nucleus is likely to be $1/2^-$ or $3/2^-$ or $3/2^+$, depending on the β values, instead of the $7/2^-$ expected for a spherical shape.

In contrast to the three levels with parallel spin and orbital angular momenta belonging to the $N = 5$ oscillator major shell, filling the three levels, $1h_{9/2}$, $2f_{5/2}$, and $3p_{1/2}$, with some neutrons which belong to the same major shell with antiparallel spin and orbital angular-momenta may not lead to deformation, in spite of the fact that these three levels may become almost degenerate around the Fermi level of certain nuclei as suggested by Fig. 4.

IV. DISCUSSION and CONCLUSIONS

A systematic study of the shell structure and the resulting possible deformation around neutron-drip-line nuclei has been carried out based on both bound and resonant neutron one-particle energies obtained from phenomenological Woods-Saxon potentials. In order to solve the eigenvalue and eigenphase problems for neutron one-particle bound and resonant levels, respectively, for a given deformed potential, the coupled differential equations obtained from the Schrödinger equation are integrated in coordinate space with correct asymptotic behavior. The coupling of a bound (or resonant) one-particle level with other levels, which are not obtained as resonant one-particle levels, is also properly taken into account in the method of the present work.

For a spherical shape with the operator of the spin-orbit potential conventionally used, weakly bound and/or low-lying resonant one-particle levels with parallel spin and orbital angular momenta tend to gather together in the energetically lower half of the oscillator major shell, while those levels with antiparallel spin and orbital angular momenta gather in the upper half. This grouping of energy levels in the spherical potential may lead to a possible deformation when neutrons start to occupy the lower half of the major shell. In contrast, the occupation of the upper half-shell by neutrons may not lead to a deformation.

A concrete result derived in the present study is that the magic number $N = 28$ disappears and $N = 50$ may disappear, while the magic number $N = 82$ may presumably survive. For a spherical shape an appreciable amount of energy gap appears at $N = 16$ and 40. Neutron-drip-line nuclei in the region of neutron number above $N = 20$, 40, and 82, namely, $N \approx$ 21–28 (island of inversion), $N \approx 41$–54, and $N \approx 83$–90,

respectively, may be quadrupole deformed, though the possible deformation depends on the proton number of the respective nuclei.

In actual nuclei it is possible that pair correlations may play an important role in the determination of the nuclear shape. It is generally understood that the pairing interaction tries to keep nuclei spherical, while the long-range part of two-body interactions such as quadrupole-quadrupole interactions is responsible for deformation. In stable nuclei deformed ground states are usually observed first after several nucleons have filled one-particle levels above the respective magic numbers. It is qualitatively understood that the presence of several nucleons makes the deformation induced by the long-range part of the interaction win against the spherical shape preferred by the pairing interaction. However, it is noted that the first two low-lying ℓ_j shells above the magic numbers of stable nuclei do not couple strongly to each other by the quadrupole-quadrupole interaction because there is a spin-flip between the two ℓ_j shells, for example, the $2p_{3/2}$-$1f_{5/2}$ shells just above $N = 28$, the $2d_{5/2}$-$1g_{7/2}$ shells above $N = 50$, and the $2f_{7/2}$-$1h_{9/2}$ shells above $N = 82$. Therefore, the deformation-driving effect in stable nuclei caused by the presence of several nucleons above the magic numbers may be weaker than in the case of neutron-drip-line nuclei. In the latter case the deformation-driving force obtained by filling neutrons in the almost-degenerate ℓ_j shells that couple strongly to each other by quadrupole-quadrupole interaction may more easily win against the spherical shape preferred by the pairing interaction. On the other hand, the effect of the pairing interaction, which tries to keep nuclei spherical, can also be different in stable and neutron-drip-line nuclei, but the difference does not yet seem to be fully pinned down.

In order to pin down a deformed shape of nuclei, measurement of both the energy of the lowest 2^+ state and the $B(E2; 2_1^+ \rightarrow 0^+)$ values in even-even nuclei is important, but observation of the spin parity of the ground state of odd-A nuclei is often decisive. For example, noting that the proton numbers $Z = 21$(Sc), $Z = 22$ (Ti), $Z = 23$ (V), and $Z = 24$ (Cr) may help to have some deformation as shown by the fact that the energies of the two lowest-lying Nilsson one-proton levels in the pf shell decrease strongly as $\beta = 0 \rightarrow \beta > 0$, the study of odd-$N$ neutron-drip-line nuclei with $N = 41$ such as $^{63}_{22}\mathrm{Ti}_{41}$ is highly desirable. In fact, the spin parity $1/2^-$ is already preliminarily assigned to the ground state of $^{65}_{24}\mathrm{Cr}_{41}$ [20]. On the other hand, the experimental study of neutron-drip-line nuclei with $N = 83$ may not be possible in the very near-future.

The possibility of deformation and the shell structure unique to neutron-drip-line nuclei, which are discussed in this article, should be duly studied by properly carrying out self-consistent HF calculations with appropriate effective interactions including pairing interaction. However, the effective interactions to be used in HF calculations of neutron-drip-line nuclei are not yet properly fixed. Moreover, such HF calculations have to be done by integrating the coupled differential equations in coordinate space with proper asymptotic behavior of wave functions for $r = R_{\max}$, at which both nuclear potential and the coupling term are negligible, instead of using the expansion of wave functions in terms of harmonic-oscillator bases or confining the system to a finite box. This kind of proper HF calculation is not yet available for neutron-drip-line nuclei. It remains to be seen whether or not neutron-drip-line nuclei with certain neutron numbers are actually deformed as suggested in the present work.

It is noted that the neutron one-particle states obtained from Nilsson diagrams for $\beta \neq 0$ are those to be recognized as band-head configurations of odd-N nuclei. Thus, rotational states, which are constructed based on these band-head states, should, in principle, be observed using a proper experimental method, and these high-spin states will have narrow widths if they appear in the low-energy region.

The systematic change of the shell structure in the spherical potential discussed in the present paper is strictly related to the characteristic features of both the weakly bound and the low-lying resonant one-particle orbits with small ℓ values. The change in the shell structure and the resulting one-particle energies in neutron-drip-line nuclei must be taken into account in shell-model calculations when the shell model is applied to neutron-drip-line nuclei.

[1] I. Hamamoto, Phys. Rev. C **69**, 041306 (2004).
[2] I. Hamamoto, Phys. Rev. C **72**, 024301 (2005).
[3] I. Hamamoto, Phys. Rev. C **73**, 064308 (2006).
[4] I. Hamamoto, Phys. Rev. C **76**, 054319 (2007).
[5] J. Dobaczewski, I. Hamamoto, W. Nazarewicz, and J. A. Sheikh, Phys. Rev. Lett. **72**, 981 (1994).
[6] A. Ozawa, T. Kobayashi, T. Suzuki, K. Yoshida, and I. Tanihata, Phys. Rev. Lett. **84**, 5493 (2000).
[7] M. Beiner, R. J. Lombard, and D. Mas, Nucl. Phys. A **249**, 1 (1975).
[8] T. Misu, W. Nazarewicz, and S. Åberg, Nucl. Phys. A **614**, 44 (1997).
[9] A. Bohr and B. R. Mottelson, *Nuclear Structure* (Benjamin, Reading, MA, 1975), Vol. II.
[10] See, e.g., R. G. Newton, *Scattering Theory of Waves and Particles* (McGraw–Hill, New York, 1966).
[11] A. Bohr and B. R. Mottelson, *Nuclear Structure* (Benjamin, Reading, MA, 1969), Vol. I.
[12] See, e.g., G. J. Kumbartzki *et al.*, Phys. Rev. C **85**, 044322 (2012).
[13] I. Hamamoto and B. R. Mottelson, Phys. Rev. C **79**, 034317 (2009).
[14] Z. Elekes *et al.*, Phys. Lett. B **586**, 34 (2004).
[15] Z. Elekes *et al.*, Phys. Lett. B **614**, 174 (2005).
[16] D. T. Yordanov *et al.*, Phys. Rev. Lett. **99**, 212501 (2007).
[17] D. T. Yordanov, K. Blaum, M. De Rydt, M. Kowalska, R. Neugart, G. Neyens, and I. Hamamoto, Phys. Rev. Lett. **104**, 129201 (2010).
[18] T. Nakamura *et al.*, Phys. Rev. Lett. **103**, 262501 (2009).
[19] P. Doornenbal and H. Scheit *et al.* (to be published).
[20] E. Browne and J. K. Tuli, Nucl. Data Sheets **111**, 2425 (2010).